2014

Low Frequency Energy Scavenging using Sub-Wave Length Scale Acousto-Elastic Metamaterial

Raiz U. Ahmed
University of South Carolina - Columbia, ahmed@engr.sc.edu

Sourav Banerjee
University of South Carolina, United States, banerjes@cec.sc.edu

Publication Info

Published in *AIP Advances*, Volume 4, Issue 11, 2014, pages #117114-.

Ahmed, R. U. & Banerjee, S. (2014). Low Frequency Energy Scavenging using Sub-Wave Length Scale Acousto-Elastic Metamaterial. AIP Advances, 4 (11), #117114. http://dx.doi.org/10.1063/1.4901915

AIP | Advances

Low frequency energy scavenging using sub-wave length scale acousto-elastic metamaterial

Riaz U. Ahmed and Sourav Banerjee

Citation: AIP Advances **4**, 117114 (2014); doi: 10.1063/1.4901915
View online: http://dx.doi.org/10.1063/1.4901915
View Table of Contents: http://scitation.aip.org/content/aip/journal/adva/4/11?ver=pdfcov
Published by the AIP Publishing

Low frequency energy scavenging using sub-wave length scale acousto-elastic metamaterial

Riaz U. Ahmed and Sourav Banerjee[a]
Department of Mechanical Engineering, University of South Carolina, Columbia, SC 29208, United States of America

(Received 3 July 2014; accepted 4 November 2014; published online 12 November 2014)

This letter presents the possibility of energy scavenging (ES) utilizing the physics of acousto-elastic metamaterial (AEMM) at low frequencies (<~3KHz). It is proposed to use the AEMM in a dual mode (Acoustic Filter and Energy Harvester), simultaneously. AEMM's are typically reported for filtering acoustic waves by trapping or guiding the acoustic energy, whereas this letter shows that the dynamic energy trapped inside the soft constituent (matrix) of metamaterials can be significantly harvested by strategically embedding piezoelectric wafers in the matrix. With unit cell AEMM model, we experimentally asserted that at lower acoustic frequencies (< ~3 KHz), maximum power in the micro Watts (~35μW) range can be generated, whereas, recently reported phononic crystal based metamaterials harvested only nano Watt (~30nW) power against 10KΩ resistive load. Efficient energy scavengers at low acoustic frequencies are almost absent due to large required size relevant to the acoustic wavelength. Here we report sub wave length scale energy scavengers utilizing the coupled physics of local, structural and matrix resonances. Upon validation of the argument through analytical, numerical and experimental studies, a multi-frequency energy scavenger (ES) with multi-cell model is designed with varying geometrical properties capable of scavenging energy (power output from ~10μW – ~90μW) between 0.2 KHz and 1.5 KHz acoustic frequencies. [http://dx.doi.org/10.1063/1.4901915]

Recent advancements in low power electronic gadgets, micro electro mechanical systems and wireless sensors have significantly increased the local power demand. To circumvent the energy demand, low power local energy harvesters are proposed for harvesting energy from different ambient energy sources. Energy harvesters utilize the ability of piezoelectric materials to generate electric potential in response to external mechanical deformation. Significant research activities on low power energy harvesters can be found in many literatures.[1–4] Key of these research activities are to introduce self-powered wireless electronics systems such that the maintenance, replacement of the old batteries and the chemical waste from conventional batteries could be avoided.[5] Microcantilever energy harvesters are the most common low power energy harvesters, where power outputs are in the range of micro Watts.[6–9] Recently, we have proposed plate type energy harvesters for high frequency applications.[10,11] Since the efficiency of the power conversion mechanism is fairly low at low frequencies, the conventional energy harvesters are designed to operate at higher frequencies (> ~3 KHz). To design low frequency energy harvesters, very recently, phononic crystal based metamaterials are introduced by creating a point defect and exploiting the physics of resonant cavity.[12] At the resonance frequency acoustic energy localizes in the cavity of the phononic crystals and Wu et al. proposed harvesting the acoustic energy using a polyvinylidenefluride (PVDF) film.[13–15] Using the comparative methodology, Lv et al.,[16] theoretically and experimentally studied an energy harvesting generator using point-defect phononic crystal coupled with piezoelectric crystal. Carrara et al.[17] proposed a metamaterial energy harvester using a parabolic acoustic mirror where wave

[a]Corresponding Author: banerjes@cec.sc.edu

guiding through an acoustic funnel was proposed.[17] Although the phononic crystal based metamaterial are promising, in all the previous studies[11–16] the harvested energy is in the range of nano Watts (~30 nW against ~10KΩ load resistance). Very recently, Zhang et al.[18] introduced a unit cell consist of a square mass connected to a square frame by four convolute folded beams. Under unit input excitation, power in nano Watts range can be harvested, against our reference load resistance 10KΩ. In spite of the fact that researchers have studied phononic-crystal and acoustic metamaterials for harvesting energy at lower frequencies, it is required to efficiently harvest energy (in μW) from sub wavelength scale size of the harvesters at lower frequencies which can be complementary to the microcantilever harvesters at higher frequencies and motivated the model presented herein.

AEMM[19] are conventionally used for stopping acoustic waves due to their low transmissibility at certain frequency ranges[18] and as a result low frequency stop band filters are designed using mass in mass systems.[20] We argue that if the filtered wave energy at the stop band frequencies are trapped inside the soft constituent of the metamaterial as dynamic strain energy, then it must be possible to recover that same energy using embedded piezoelectric wafers (figure 1(a)). Hence, coupling two different physics in a single phenomenon we can make the AEMM bimodal in applications. The possibility of simultaneous wave filtering and energy harvesting was first mentioned by Gonella et al.[21] in 2009, however it was not experimentally proven. In AEMM, the soft material is used as a host matrix to house the heavy mass. The trapped wave oscillates inside the matrix differently at different modes. Maximum power can be harvested while the piezoelectric wafer is strained inside the matrix due to the local resonance of the embedded mass. In addition we also report two additional cases, structural resonances and effect of local matrix splashing, where significant energy can be harvested through appropriate design and strategic placement of smart materials. Thus we further propose a multi-cell energy scavenger model with the ability to harvest energy at multiple frequencies. Our model is motivated to satisfy four requirements and overcome three draw backs that dominates in the existing models, they are: 1) simultaneous wave filtering and energy harvesting; 2) operate at low frequency, <3 KHz; 3) Significantly higher and maximized power output; 4) allow energy harvesting at multiple frequencies using single unit cell.

To illustrate the concept, we considered a three-dimensional unit-cell model shown in figure 1(b). The unit cell is a rectangular ~36.5 mm X ~36.5 mm X ~14 mm prism consisting of a rectangular aluminum frame with a cylindrical matrix inside. A spherical heavy core made of lead (Pb) is encapsulated inside the matrix. Diameter of the core mass (D_m) and the matrix (D_M) are ~12.5 mm and ~25 mm, respectively. Young's modulus of aluminum, lead and matrix are ~68.9 GPa, ~13.5 GPa and ~0.98 MPa, respectively. To convert the trapped strain energy into electrical potential, a piezoelectric wafer (ϕ~7 mm, thickness = ~0.5 mm, mass = ~0.16 gm) is embedded inside the matrix at the center between the lead core and the cavity wall (figure 1(a)). The unit-cell model of the metamaterial could be exhibited as conventional one-dimensional spring-mass system.[22–25] The displacement of the core mass responds harmonically[26] in response to the harmonic load $U(t) = Re\left(U_0 e^{-i\omega t}\right)$. Acknowledging the equation of motion and balancing the linear momentum of the system, we attain the dynamic effective mass of the microstructures viz.

$$M_{eff} = M_0 + \frac{2Km_1}{2K - m_1\omega^2} + \frac{2Km_2}{2K - m_2\omega^2} \tag{1}$$

Where, M_0, m_1 and m_2 are the masses of aluminum frame, lead core and piezoelectric wafer, respectively. K=~1 KPa the spring constant for the matrix component. Assuming thickness-polarized piezoelectric state, the piezoelectric charge density is given by, $D_3 = d_{33}T_3 + \varepsilon_{33}E_3$, where T_3 is the total compressive stress acted on the piezoelectric wafer. ε_{33} (=1500*8.854 pF/m), d_{33} (=593 pm/V) and $E_3 = V_0/h_p$ are the permittivity, piezoelectric charge constant and electric field strength, respectively, where, h_p is the thickness of the wafer and V_0 is the voltage output. Due to resonance, the total compressive force (F_3) was first calculated and then the average stress ($T_3 = F_3/A_p$) was computed on the wafer, where, $A_p = \pi r_p^2$ and r_p is the radius of the wafer. Next the electric charge density was calculated using the Gauss's law $q = \int \mathbf{D}.\mathbf{n}dA_p$. Time derivative of electric charge density is the current generated by the wafer. Following the assumptions and few mathematical steps, expressions for the dynamic voltage (V_0) output, Frequency Response Function (FRF) and the

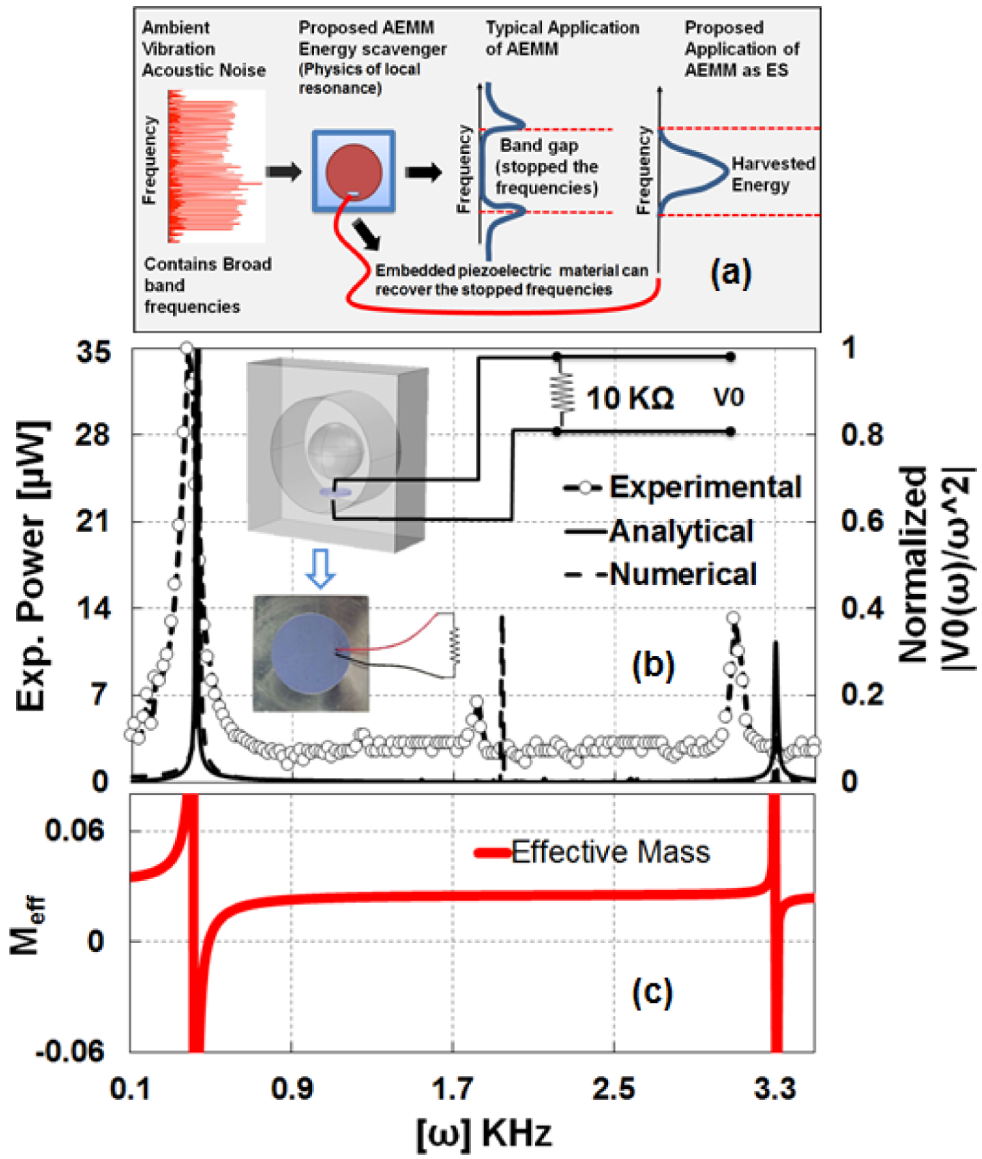

FIG. 1. (a) A dual mode depiction of AEMM (b) Analytically, numerically and experimentally obtained dynamic FRF and output power (μW) against 10 KΩ load resistance. (c) Analytically computed dynamic effective mass: correlation between peak harvesting frequency and frequency of negative mass.

power output (P_0) are

$$P_0(\omega) = \frac{[V_0(\omega)]^2}{R_0} \qquad V_0(\omega) = \frac{i\omega C_1 R_0 U_0}{1 - i\omega C_2 R_0} \qquad FRF = \left|\frac{V_0(\omega)}{\omega^2}\right| \tag{2}$$

$$\text{Where, } C_1 = -\frac{2d_{33}M_e}{r_p} \qquad C_2 = -\frac{2\pi r \varepsilon_{33}}{h_p} \qquad M_e = 2 - \frac{2K}{2K - m_1\omega^2} + \frac{2K}{2K - m_2\omega^2}$$

Here in this letter, we used, $U_0 = 1\ mm$, the excitation amplitude of the system, $R_0 = 10\,K\Omega$, the external resistive load. Resistive load affects the current and at certain load resistance, the circuit harvests maximum power[11,27] due to resonance. Higher acceleration is capable of harvesting higher power,[28] thus FRF function is presented in this letter to normalize such effect. In this study the fundamental possibility of designing an AEMM based energy scavenger is presented and extensive analysis revealing the effect of ground acceleration and external load resistance are omitted.

Dynamic effective mass[22] (figure 1(b)) of the system is found to be negative at ~0.42 KHz and ~3.3 KHz. This also implies[18] that wave energy is trapped inside the soft matrix and cannot be transmitted through the structure.[24,25] Consequently, the embedded wafer is stressed and maximum FRF is obtained at the local resonance frequencies (figure 1(a)). Two dominant peaks are observed, the first peak results from the local resonance of the core mass and the second peak is due to the resonance of the wafer itself.

Numerical computation supports the analytical argument with maximum FRF at ~0.43 KHz and ~3.31 KHz. Numerical study was performed using COMSOL multiphysics in 3-dimensional (3D) using 4-noded tetrahedral elements. Element size was 1/4 times of the wavelength in respective constituent at the highest frequency (~3 KHz). Frequency domain analysis is performed with vertical displacement excitation $U_0 = 1\ mm$. Despite the fact that the numerical analysis is performed using a 3D model and the analytical study is performed using a 1-dimensional (1D) spring-mass model, resonance frequencies are in very close agreement. In both occasions (resonance of the core mass and the wafer) the piezoelectric material encounters high compressive stress and produces maximum electric potential (figure 2(a), 2(b)). On contrary, two different cases of low FRF at off-resonance frequencies (e.g. ~0.98 KHz & ~1.47 KHz) are shown in figure 2(c) & 2(d). At ~0.98 KHz, the core mass moved towards the wafer but the matrix flows along the frame. Hence, the matrix adjacent to the wafer has a tendency to stream toward fringe matrix and distance between two masses is decreased. Although there is a relative movement, the lead ball is unable to create considerable stress on the wafer and negligible power is harvested. At ~1.47 KHz, wave energy

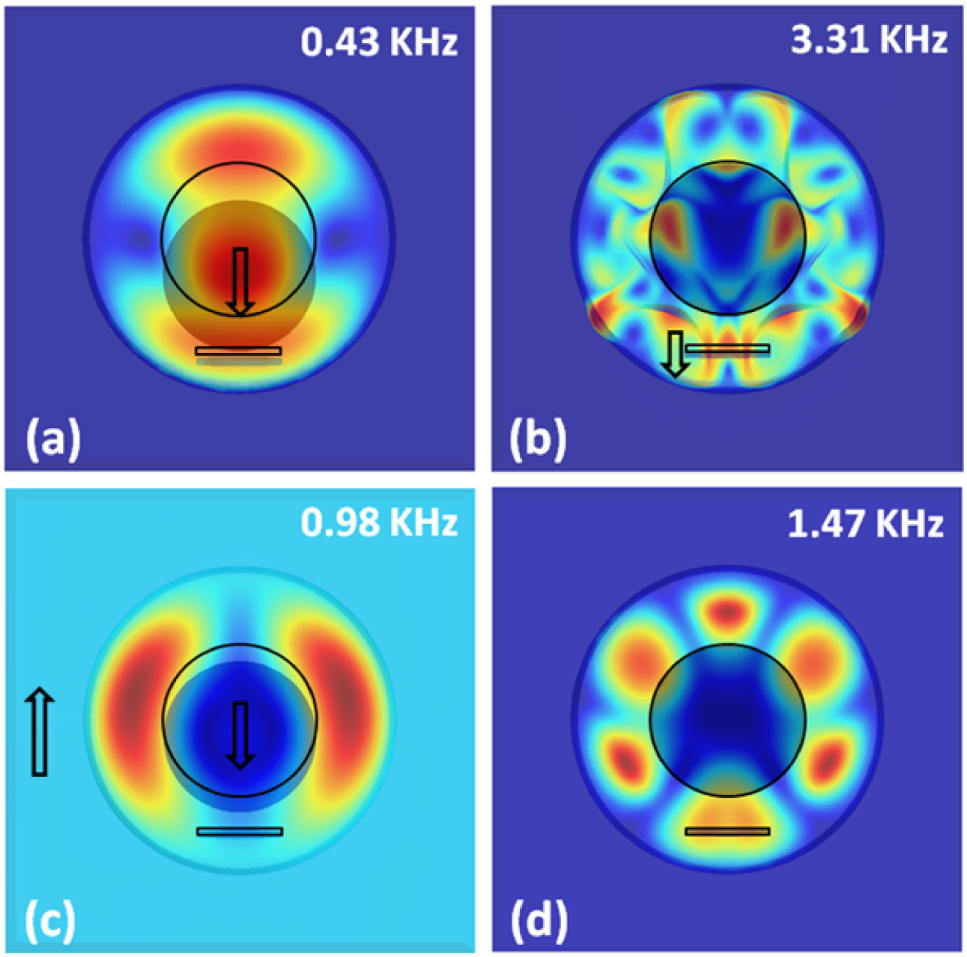

FIG. 2. Displacement patterns in an unit cell at (a) ~0.43 KHz (b) ~3.31 KHz (c) ~0.98 KHz and (d) ~1.47 KHz.

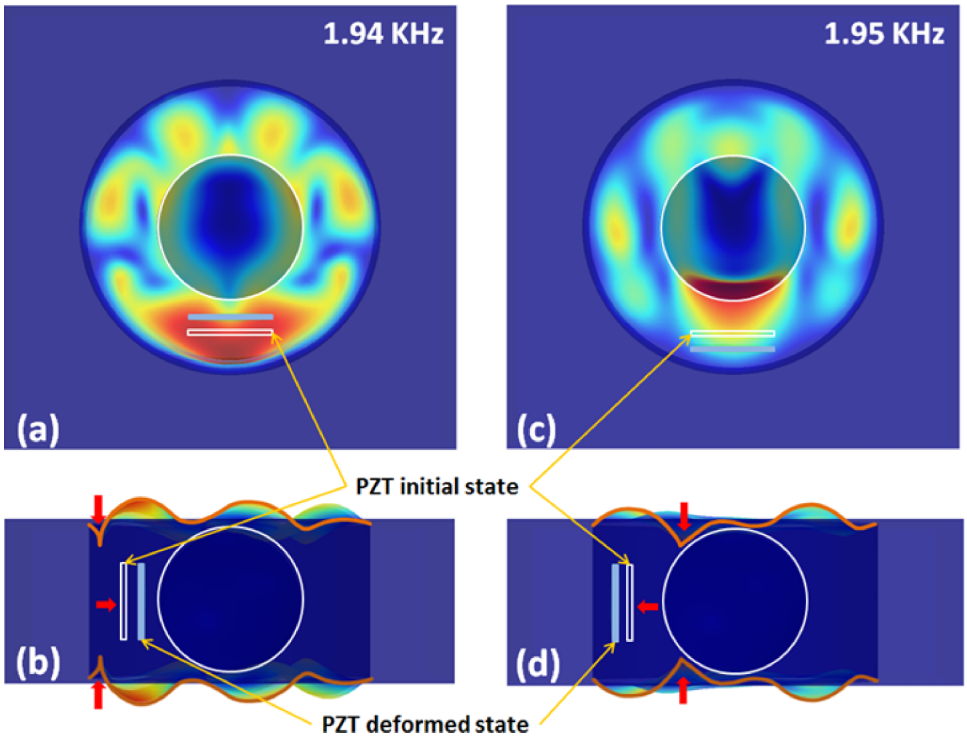

FIG. 3. Matrix splashing phenomenon in unit cell model at the transition between ~1.94 KHz and ~1.95 KHz. Displacement plots at ~1.94 KHz (a) front view (b) side view with surface outlines. Displacement plots at ~1.95 KHz (c) front view (d) side view with surface outlines.

stays trapped inside the matrix as dynamic oscillation, while the core and the wafer are stationary. This phenomenon also results negligible harvested energy. An additional possibility of harvesting energy at ~1.94 KHz (figure 1(a)) was found, which is not intuitive and was also not observed from the 1D analytical model. In this letter, it is commented that the consequence of matrix splashing, contained between the core mass and the wafer, the modal inflection between ~1.94 KHz and ~1.95 KHz causes the harvesting (figure 3). Oscillation of the matrix between the wafer and the heavy mass which is stationary causes the wafer to deform and produces electric potential.

Next, the experimental study was performed using vibration exciter (type 4809), sine-random generator (type 1024) and a power amplifier (type 2706) from Bruel & Kjaer Instruments. The vibration exciter was used to hold the proposed model and the sine-random generator regulated the frequency ($\sin(\omega t)$) and amplitude ($U_0 = 1\ mm$) of the vertical excitation as shown in figure 4. The experimental approach reinforces (figure 1(a)) the analytical and numerical results with maximum harvested energy at ~0.37 KHz (~35μW) and ~3.1 KHz (~15μW). In our experimental study, possible fabrication error and limitation of the instrumentation may have caused little shifts in the FRF peaks compared to the numerical and analytical solution. This may occur from the imperfect alignment of the piezoelectric wafer with respect to the core mass (where, figure 3 shows the perfect alignment). However, this is a positive sign and open problem of research to study the geometrical placement of the wafer inside the matrix for optimizing energy output and shift the power peaks. The harvested power up to ~36 μW against ~10 KΩ resistive load is significantly higher than the power generated (in nW range) by phononic crystal based energy harvesters.[13] The FRF peak at ~1.94 KHz, suggested by the numerical computation is weakly observed in the experimental power output. Again such mismatch could be the result of imperfect alignment of the piezoelectric wafer.

Since the dynamic effective mass of the system strongly depends on the mass of the core resonator, we further propose a multi-frequency scavenging model. The proposed model consists of multiple (five) cells with linearly varying core mass in each cell (figure 5(a)). Mirror construction of the multi-cell wings is fabricated to avoid vibration instability during the dynamic operation.

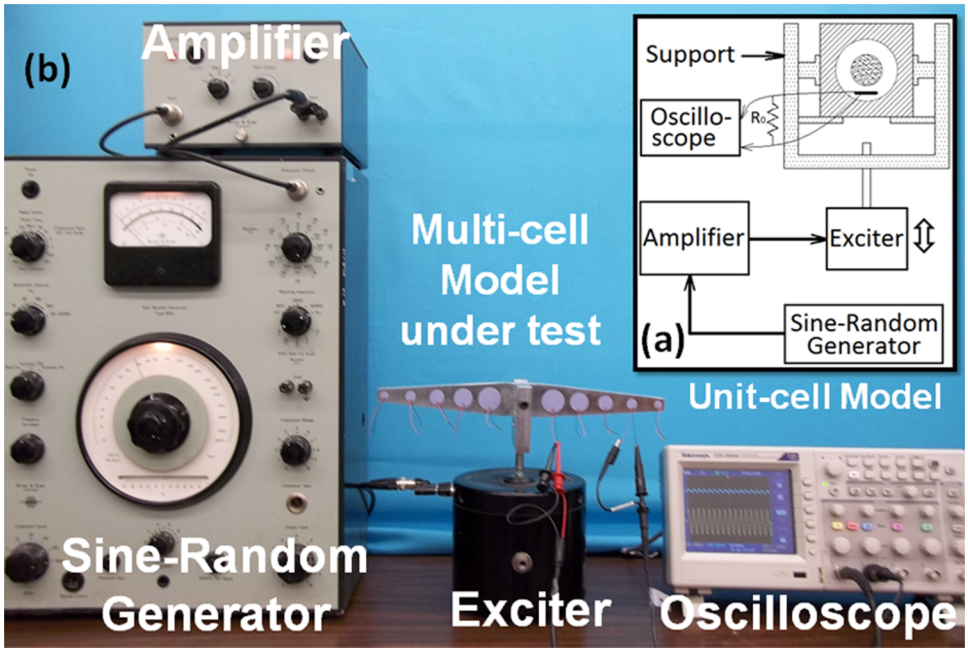

FIG. 4. (a) Schematic diagram of the experimental arrangement for the unit cell metamaterial at the top-right; (b) Actual experimental arrangement for the multi-cell acoustoelastic metamaterial.

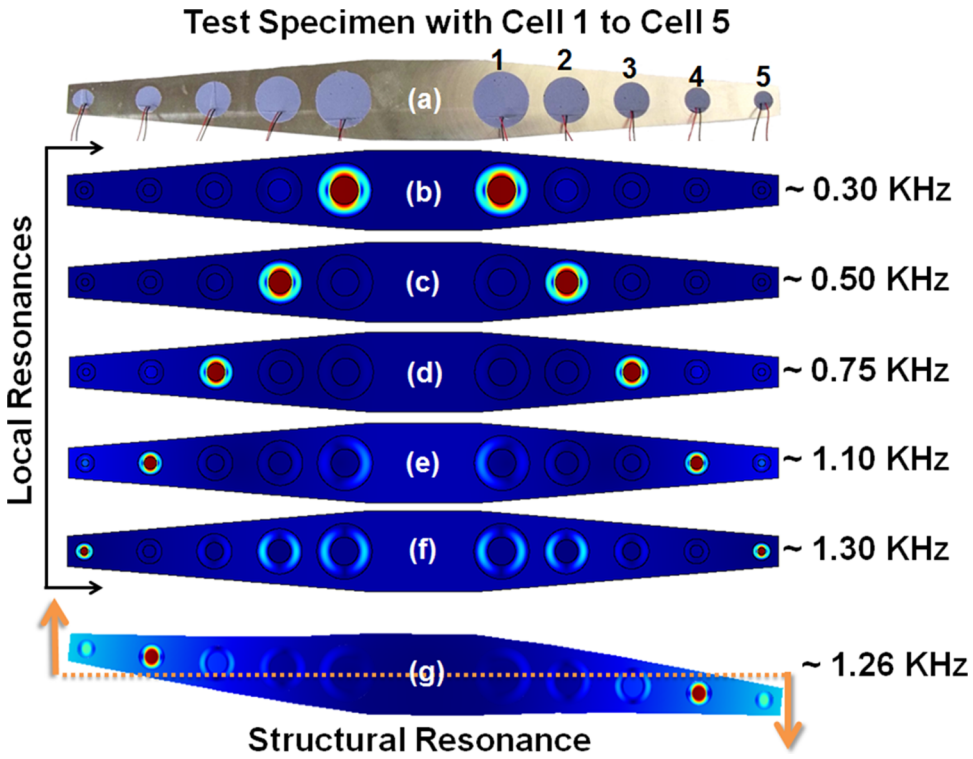

FIG. 5. (a) Multi-cell metamaterial model. Displacement patterns obtained through numerical simulation at (b) ~0.30 KHz (c) ~0.50 KHz (d) ~0.75 KHz (e) ~01.10 KHz (f) ~1.30 KHz. (g) structural resonance at ~1.26 KHz.

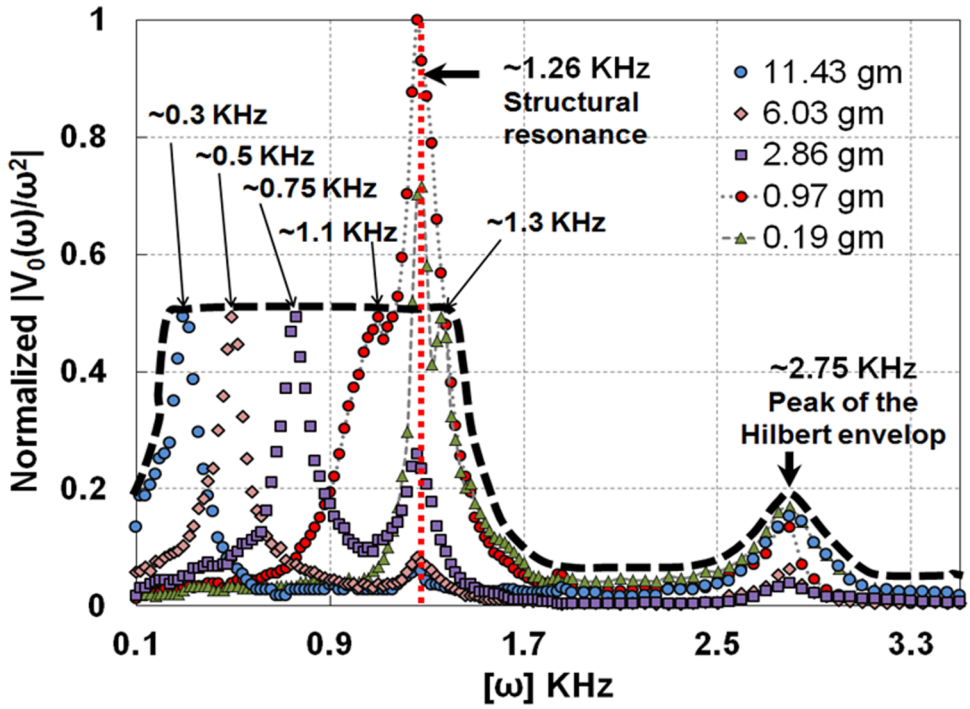

FIG. 6. Normalized experimental power output from multiple frequencies using multi-cell metamaterial model. Scavenged energy ranges between ~10μW - ~90μW, between frequencies ~0.2 KHz – ~1.5 KHz inclusive all local, structural and matrix splashing phenomena. Additional peak at ~2.75 KHz was observed due to wafer resonance.

The proposed model is linearly tapered toward smaller cells and center-to-center spacing between cells are constant. Here a special measure was taken to keep the wafer inside the matrix in perfect alignment.

Numerical and experimental investigations suggests that wave energies at different frequencies are trapped (figure 5(b)-5(f)) and can be harvested (figure 6) using the proposed model. From cell 1 with heaviest core mass (11.43 gm, D_m=12.5 mm, D_M=25 mm), the peak harvested power (against 10KΩ, ~5μW) can be obtained at ~0.32 KHz. Additionally, it was found that the peak energy can also be harvested at other frequencies, e.g., ~0.50 KHz (~34μW), ~0.76 KHz (~35μW), ~1.1 KHz (~22μW) and ~1.38 KHz (~11μW) from the cells with decreased core masses. Mass and diameter (D_m) of the core masses are in cell 2: ~6.03 gm, ~10.2 mm, cell 3: ~2.86 gm, ~7.9 mm, cell 4: ~0.97 gm, ~5.6 mm and cell 5: ~0.19 gm, ~3.3 mm, respectively and in all cells D_M=2 D_m. In our experiment, the cell 2 and the cell 3 harvested maximum power from the local resonances, which reveals that there is best geometric ratio of the matrix diameter (with fixed matrix property) to the wafer diameter, which harvests maximum energy at the local resonances. From this study, it was found that the ratio would be ~2.5. In figure 6 it can be seen that the FRF peaks between ~2.6 KHz - ~3.1 KHz are consistent among all the cells because the mass of the piezoelectric wafers are similar in cell 1 – cell 4 and approximately ~60% in cell 5. In figure 6 the FRF peaks are normalized with respect to each respective cell at the local resonances. If all possible core masses are integrated in one structure, it is demonstrated that the multi-frequency energy scavenging using a multi-cell model is possible. To illustrate further, the voltage output from multiple cells at ~0.30 KHz and ~1.10 KHz are plotted in figure 7, which confirms that at ~0.30 KHz and ~1.1 KHz, the energy can be harvested from the cells with core mass ~11.43 gm and ~0.97 gm, respectively. Figure 5(g) shows an additional FRF peaks at ~1.26 KHz, which is consistent among all the cells but having varied power amplitude. Figure 6 shows that the cell 4 and cell 5 generated maximum power at ~1.26 KHz. The peak can be explained from the figure 5(g), which shows the effect of structural resonance. However, the amount of energy that can be harvested from each cell greatly varies depending on their respective location in the structure.

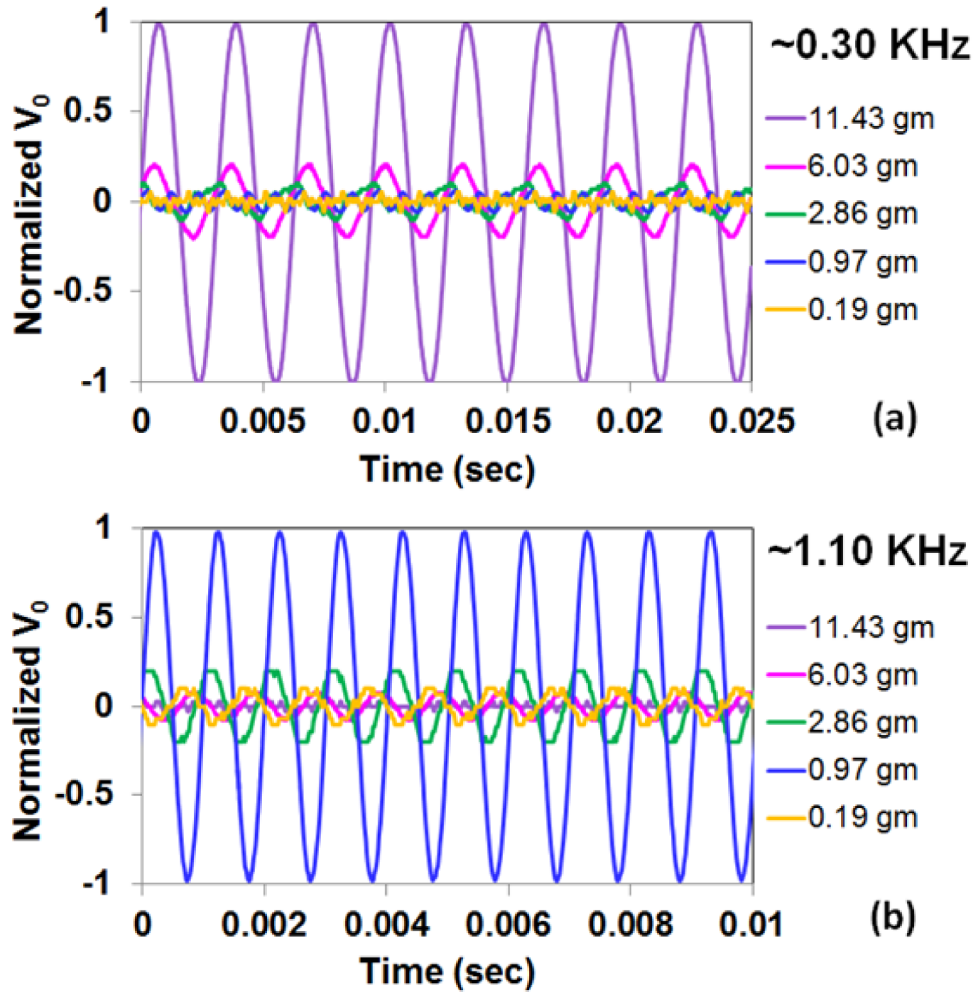

FIG. 7. Normalized voltage output at (a) ~0.3 KHz and (b) ~1.1 KHz with different core mass in each cell.

CONCLUSION

This letter demonstrates that an acousto-elastic metamaterial (AEMM) can be transform into a sub wavelength scale multi-frequency energy scavenger. They are complementary to the microcantilever and phononic crystal based harvesters at respectively high and low frequency applications. It is shown that by setting a piezoelectric wafer inside the soft matrix of AEMM, significant electric potential can be recovered and the amount of power that can be harvested, is significantly higher (from ~10μW to ~90μW against 10KΩ) compared to the existing phononic crystal based metamaterial harvesters (~30nW against 10KΩ). Validation, through analytical, numerical and experimental study, a multi-cell model for multi-frequency energy scavenging is proposed which is a heuristic design to demonstrate the concept, but any application specific structure can be manufactured at sub wave length scale by applying the similar physics. It is shown that the systematic selection of the core mass, placement of piezoelectric wafer and coupling local, structural and matrix resonance in a multi-cell system could result a broadband energy scavenging device.

ACKNOWLEDGMENT

Authors would like to acknowledge the financial support from the Office of Vice President of Research at the University of South Carolina. Authors are thankful to Prof. Juan Caicedo and

Prof. Anthony P. Reynolds with Department of Civil and Environmental Engineering and Department of Mechanical Engineering at the University of South Carolina, respectively for providing instrumental and material support for the experimental studies.

[1] S. P. Beeby, M. J. Tudor, and N. M. White, Measurement Science and Technology **17**(12), R175 (2006).
[2] S. R. Anton and H. A. Sodano, Smart Materials and Structures **16**(3), R1 (2007).
[3] S. Priya, Journal of Electroceramics **19**(1), 167–184 (2007).
[4] K. A. Cook-Chennault, N. Thambi, and A. M. Sastry, Smart Materials and Structures **17**(4), 043001 (2008).
[5] K. A. Cunefare, E. A. Skow, A. Erturk, J. Savor, N. Verma, and M. R. Cacan, Smart Materials and Structures **22**(2), 025036 (2013).
[6] W. J. Choi, Y. Jeon, J. H. Jeong, R. Sood, and S. G. Kim, Journal of Electroceramics **17**(2-4), 543–548 (2006).
[7] W. Zhuo and Y. Xu, Applied Physics Letters **90**(26), 263512-263512-263513 (2007).
[8] D. Shen, J.-H. Park, J. Ajitsaria, S.-Y. Choe, H. C. W. III, and D.-J. Kim, Journal of Micromechanics and Microengineering **18**(5), 055017 (2008).
[9] A. Erturk and D. J. Inman, Smart Materials and Structures **18**(2), 025009 (2009).
[10] S. Banerjee, JP Journal of Solids and Structures **5**(2), 75–105 (2011).
[11] R. Ahmed and S. Banerjee, Journal of Engineering Mechanics (In press) (2014).
[12] Z. Chen, B. Guo, Y. Yang, and C. Cheng, Physica B: Condensed Matter **438**(0), 1–8 (2014).
[13] L.-Y. Wu, L.-W. Chen, and C.-M. Liu, Applied Physics Letters **95**(1), - (2009).
[14] L.-Y. Wu, L.-W. Chen, and C.-M. Liu, Physics Letters A **373**(12–13), 1189–1195 (2009).
[15] L.-Y. Wu, L.-W. Chen, and C.-M. Liu, Physica B: Condensed Matter **404**(12–13), 1766–1770 (2009).
[16] H. Lv, X. Tian, M. Y. Wang, and D. Li, Applied Physics Letters **102**(3), - (2013).
[17] M. Carrara, M. R. Cacan, M. J. Leamy, M. Ruzzene, and A. Erturk, Applied Physics Letters **100**(20), - (2012).
[18] S. Zhang and J. H. Wu, presented at the ASME 2013 International Mechanical Engineering Congress and Exposition, 2013 (unpublished).
[19] Z. Liu, X. Zhang, Y. Mao, Y. Y. Zhu, Z. Yang, C. T. Chan, and P. Sheng, Science **289**(5485), 1734–1736 (2000).
[20] P. Sheng, X. X. Zhang, Z. Liu, and C. T. Chan, Physica B: Condensed Matter **338**(1–4), 201–205 (2003).
[21] S. Gonella, A. C. To, and W. K. Liu, Journal of the Mechanics and Physics of Solids **57**(3), 621–633 (2009).
[22] K. T. Tan, H. H. Huang, and C. T. Sun, Applied Physics Letters **101**(24), - (2012).
[23] Z. Liu, C. T. Chan, and P. Sheng, Physical Review B **71**(1), 014103 (2005).
[24] H. H. Huang, C. T. Sun, and G. L. Huang, International Journal of Engineering Science **47**(4), 610–617 (2009).
[25] A. P. Liu, R. Zhu, X. N. Liu, G. K. Hu, and G. L. Huang, Wave Motion **49**(3), 411–426 (2012).
[26] G. W. Milton and J. R. Willis, Proceedings of the Royal Society A: Mathematical Physical and Engineering Science **463**(2079), 855–880 (2007).
[27] S. Priya and D. J. Inman, Springer **ISBN: 978-0-387-76463-4**. (2009).
[28] A. Erturk and D. J. Inman, Smart Mater Struct. **18** (025009) (2009).